Pergamon

Chemical Engineering Science, Vol. 49, No. 21, pp. 3565–3586, 1994

0009–2509/94 $7.00 + 0.00

0009–2509(94)00168–5

STEADY INCOMPRESSIBLE LAMINAR FLOW IN POROUS MEDIA

SHIJIE LIU, ARTIN AFACAN and JACOB MASLIYAH†
Department of Chemical Engineering, University of Alberta, Edmonton, Canada T6G 2G6

(*First received* 25 *January* 1994; *accepted in revised form* 10 *May* 1994)

Abstract—Steady incompressible laminar flow in porous media is studied. The volume averaging technique is revisited resulting in a new averaging approach to the pressure gradient term. The difference between the traditionally obtained volume averaged equation for very small flow rate and Brinkman's equation is resolved. The Kozeny–Carman theory is modified. By including a two-dimensionally modelled tortuosity and curvature ratio as well as pore cross-sectional area variation, a new semi-empirical equation for the pressure drop for flow through porous media is obtained. The pressure drop dependence on the porosity ε for Darcy's flow region is established as $\varepsilon^{-11/3}(1-\varepsilon)^2$ as opposed to $\varepsilon^{-3}(1-\varepsilon)^2$ in the original Kozeny–Carman's theory. A modified Reynolds number is also defined. The regions of Darcy's flow and Forchheimer's flow are unified. The wall effects are incorporated into the unified pressure drop equation. The final form of the normalized pressure drop equation for a one-dimensional medium is given by

$$-\frac{\Delta p'}{L}\frac{d_s'^2\,\varepsilon^{11/3}}{\mu U(1-\varepsilon)^2} = f_v = 85.2\left[1+\frac{\pi d_s}{6(1-\varepsilon)}\right]^2 + 0.69\left[1-\frac{\pi^2 d_s}{24}(1-0.5d_s)\right]Re_m\frac{Re_m^2}{16^2+Re_m^2}$$

for $d_s = d_s'/D < 0.75$. Here f_v is the normalized pressure drop factor, $-\Delta p'$ is the pressure across a fixed thickness L of the porous bed, ε is the porosity, d_s' is the equivalent spherical particle diameter, D is the bed diameter, U is the superficial velocity or fluid discharge rate, μ is the dynamic viscosity of the fluid and Re_m is the modified Reynolds number. The one-dimensional pressure drop equation is also modified to give a shear factor for use with the volume averaged Navier–Stokes equation and it is given as

$$F = \frac{(1-\varepsilon)^2}{4\varepsilon^{11/3}d_s^2}\left\{85.2\left[1+\frac{\pi d_s}{6(1-\varepsilon)}\right]^2 + 0.69\left[1-\frac{\pi^2 d_s}{24}(1-0.5d_s)\right]Re_v\frac{Re_v^2}{16^2+Re_v^2}\right\}$$

where F is the shear factor and Re_v is the local modified Reynolds number. The semi-theoretical model was tested with available and new experimental pressure drop data for packed beds. Further comparison was made with experimental pressure drop data for flow in a fibrous mat. The model was found to correlate well for the whole range of Reynolds number, wall effects and porosity studied.

1. INTRODUCTION

Flow in porous media plays an important role in many science and engineering fields. The application of flow in porous media can be found in: reservoir engineering, biomechanics, geophysics, hydraulics, soil mechanics and in chemical, aeronautical and petroleum engineering. Owing to its complexity, flow in porous media has been studied by and large, through direct experimentation. Computational flow simulations have been largely confined to zero flow strength and to geometrically simple ordered porous media.

A one-dimensional empirical model for flow in porous media was introduced by Darcy (1856) with a simple linear relation between pressure gradient and flow rate that has a constant permeability. Darcy's law can be expressed as

$$u' = -\frac{k}{\mu}\nabla p' \qquad (1)$$

where u' is the superficial fluid flow velocity (or discharge rate), k is the permeability of the porous medium taken as a constant, μ is the dynamic viscosity of the fluid and $\nabla p'$ is the pressure gradient in the flow direction. Equation (1) has been generalized and it is widely used for multi-dimensional flows. Darcy's law lacks the flow diffusion effects, i.e., $\nabla^2 u'$ term, and hence it is not valid at the interface of a porous medium—solid or porous medium—free flow.

Brinkman (1949) added a diffusion term to the Darcy's law, leading to

$$\nabla p' = -\frac{\mu}{k}u' + \tilde{\mu}\nabla^2 u' \qquad (2)$$

where $\tilde{\mu}$ is an effective viscosity. He also found that the effective viscosity $\tilde{\mu}$ should be the same as the fluid viscosity μ in order to accomodate the available experimental data. Brinkman's equation becomes

$$\nabla p' = -\frac{\mu}{k}u' + \mu\nabla^2 u'. \qquad (3)$$

Equation (3) has been used and generalized for multi-dimensional flows by many investigators as the governing flow equation for flow through porous media including Neale *et al.* (1973) and Nandakumar and

†Author to whom correspondence should be addressed.

Masliyah (1982). Brinkman's equation is, like Darcy's law, inertia-free and hence valid only for very weak flows. A few theoretical studies gave some heuristic accountability for Brinkman's equation by using volume averaging of the Navier–Stokes equations for flow in porous media (Whitaker, 1966; Slattery, 1969; Lundgren, 1972). However, these studies gave different viscosities to the Brinkman's equation. The traditional volume averaging technique assumed that the pressure (Lundgren, 1972) or the pressure gradient (Whitaker, 1966; Slattery, 1969) inside the solid material was zero and would influence the flow in the pores.

To account for the non-linear behaviour of the flow in porous media, Forchheimer (1901) hypothesized that the pressure drop for flow in a packed bed results from both viscous and inertial effects, and postulated that

$$-\nabla p' = \alpha u' + \beta u'^2 \tag{4}$$

where α and β are constants, and like the permeability k, they depend on the structure of the porous medium. The Forchheimer hypothesis has been generally accepted as an extension to the Darcy's law for high flow rates. The Forchheimer relation has attracted much attention in the literature. The qualitative relation was heuristically obtained by many authors through various means. Among others, Blick (1966) used a model of a bundle of parallel capillary tubes with orifice plates spaced along the tubes. A static balance of forces was applied to obtain a Forchheimer-type relation. Coulaud *et al.* (1988) obtained the Forchheimer relation by correlating their own numerical results on flow across bundles of cylinders arranged in a regular pattern. These authors obtained a deterministic equation where the coefficients can be determined without the need for direct experiments. Other investigators used the continuum approach to arrive at the Forchheimer relation, for example Dullien and Azzam (1973), Barak and Bear (1981) and Cvetkovic (1986). In general, the continuum approach was used as a means to explain the physics behind the Forchheimer relation and not to quantify the pressure drop for flow through porous media. In other words, the Forchheimer equation is not uniquely obtainable by averaging theory (Ruth and Ma, 1992). To quantify the pressure drop for flow through porous media, the process involved with the continuum approach would be formidable.

Equations (1), (3) and (4) contain unknown constants k, α and β that are properties of the porous medium. Hence, the above-mentioned equations are strictly speaking qualitative expressions and have limited scope of utility. Kozeny (1927) introduced a model that represents porous media as bundles of straight passages. The Kozeny's theory was subsequently revised by Carman (1937). With the Kozeny–Carman theory, the porous medium properties can be accounted for in the pressure drop–flow rate relationship. One-dimensional pressure drop of flow through porous media has been correlated semi-empirically by various investigators based on Kozeny's theory and Forchheimer's hypothesis. The first of such approaches is well documented by Carman (1937). The most notable study is by Ergun (1952). Together, they formed the basis for most of the more recent investigations. The correlation given by Ergun (1952) received most attention and has been termed the Ergun equation. It can be written as

$$-\frac{\Delta p'}{L}\frac{d_s'\varepsilon^3}{\mu u'(1-\varepsilon)^2} = 150 + 1.75\frac{d_s' u'\rho}{(1-\varepsilon)\mu} \tag{5}$$

where $\Delta p'$ is the pressure drop, L is the apparent length parallel to the flow, d_s' is the equivalent spherical diameter of a representative unit solid element (particle), ε is the porosity and ρ is the density of the fluid. A similar equation was also theoretically derived by Irmay (1958), who assumed a specific pore structure. The Ergun equation has been revised by various investigators, to name a few, Wentz and Thodos (1963), Handley and Heggs (1968), Tallmadge (1970), Hicks (1970) and Jones and Krier (1983). A recent and more accepted correlation (modified Ergun equation) is given by MacDonald *et al.* (1979). The Ergun equation has also been used in estimating the permeability of unconsolidated porous media (Dullien, 1979). However, MacDonald *et al.* noted that the Ergun equation is valid over a certain porosity range and it is not valid for the entire range of porosity. This may be attributed to the oversimplification in the Kozeny–Carman theory in which parallel straight passages were assumed as the internal structure of a porous medium.

With the advent of the volume averaging technique, progress in modelling multi-dimensional flows through porous media has been made in recent years. The volume averaging technique was established by Whitaker (1966), Slattery (1969), Bear (1972), Lundgren (1972) and Bachmat and Bear (1986). The volume averaging technique results in an excess shear loss term in the volume averaged Navier–Stokes equation. The excess shear loss term was modelled by Du Plessis and Masliyah (1988, 1991) with an idealized macrostructure of a parallel torturous square passage inside a porous medium. Du Plessis and Masliyah's model puts the volume averaged Navier–Stokes equation into use to study the flow in a porous medium by capturing the flow behaviour inside a porous medium structure in an average sense rather than serving only as a proof to the Brinkman's equation and/or Darcy's law. The Du Plessis–Masliyah model was further improved by Du Plessis (1992) to allow for an agreement with the Ergun equation at a porosity of 0.5. However, when the flow strength is zero, the volume averaging technique as was traditionally used does not yield the exact form of Brinkman's equation (3), that best describes the experimental data. The excess shear loss term was also modelled by Ma and Ruth (1993) with a periodic-sudden-diverging-converging channel.

Although there is a vast amount of literature for flow through porous media, the wall effect has received little attention. The first recognition of the wall

effect was made by Carman (1937). He analysed the wall effect by considering the extra wetted surface area presented to the flow. His argument was partially utilized in correlating experimental results by Metha and Hawley (1969), Reichelt (1972) and Fand and Thinakaran (1990). These authors considered the extra wetted surface area to have identical effects as the particle surface area for all the terms by revising the equivalent diameter of the flow passage. However, no acceptable theory or experimental correlation has been established for the wall effect.

The objectives of this study are: (a) to examine the volume averaging technique and attempt to resolve the difference between the experimentally observed Brinkman equation and the volume averaged Navier–Stokes equation for weak flows in porous media; (b) to revisit the Kozeny–Carman theory and likewise heuristic arguments are used to derive an improved Ergun equation-type relationship; (c) to study the wall effect in a more systematic manner; and (d) to compare with available and new experimental data obtained in this study.

2. VOLUME AVERAGED GOVERNING EQUATIONS

For steady incompressible flow of a Newtonian fluid in porous media, a geometrical characteristic length a and a characteristic flow velocity U are used to render the flow variables dimensionless. Some of the variables and parameters, as an example, for flow in a cylindrical pipe containing porous media, are:

$$\mathbf{v} = \mathbf{v}'/2U, \qquad p = ap'/(2\mu U), \qquad r = r'/a, \qquad x = x'/a, \qquad Re = 2a\rho U/\mu \quad (6)$$

where $\mathbf{v}$ is the pointwise superficial flow velocity vector, p is the pressure, r is the radial coordinate, x is the axial coordinate and Re is the pipe Reynolds number. The primed variables are the corresponding dimensional quantities.

A single-phase, Newtonian, incompressible fluid flow with constant physical properties will be considered. The Navier–Stokes equation governing the flow is given as

$$Re\,\nabla\cdot(\mathbf{v}^*\mathbf{v}^*) + \nabla p^* - \nabla^2\mathbf{v}^* = 0 \quad (7)$$

where the superscript * is used to indicate a local microscopic value.

The porous medium is assumed to be isotropic and all the pores are interconnected and furthermore, without dead ends. Owing to the complexity of the structure inside a porous medium, the actual flow velocity inside the pores is not of importance. Instead, the superficial velocity (or discharge rate) can give a good estimate of the flow behaviour. In order to obtain the governing equation in terms of the superficial velocity, the Navier–Stokes equation is averaged within a representative elementary volume (REV) [see Bear (1972) and Du Plessis and Masliyah (1988)]. Figure 1 shows a sketch of the REVs for an orderly packed bed of spheres on the left and an orderly consolidated matrix on the right.

Some of the definitions and the volume averaging rules can be summarized as follows:

(a) for a given physical characteristic quantity ϕ,

$$\phi = \frac{1}{V}\int_V \phi^*\,\mathrm{d}V = \varepsilon\phi_\varepsilon \quad (8)$$

where ϕ^* is the local microscopic property, ϕ_ε is its corresponding intrinsic phase averaged value (local macroscopic), ϕ is its superficial or average value based on the whole volume and V is the volume of the representative elementary volume within which the averaging is made. For example, $\mathbf{v}$ is the superficial velocity (macroscopic), $\mathbf{v}^*$ is the interstitial velocity (local microscopic) and $\mathbf{v}_\varepsilon$ is the intrinsic phase average interstitial velocity (local macroscopic). An REV is the minimum space volume located anywhere inside the porous medium domain within which the measurable characteristics of the porous medium remain constant. For example, for randomly packed beds of spherical particles, the REV should be at least the

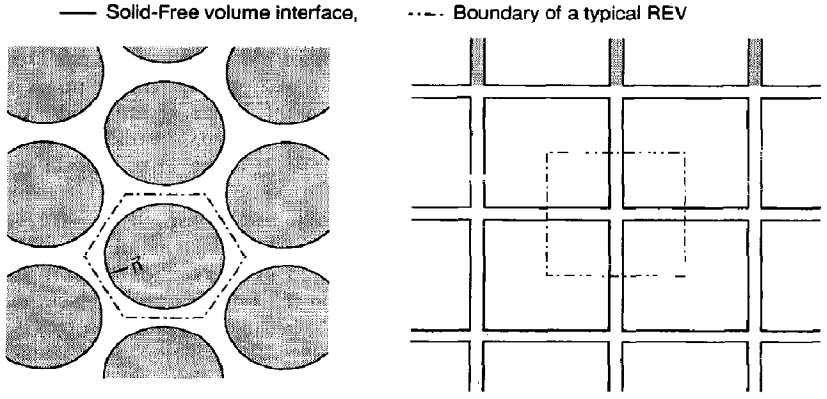

Fig. 1. A sketch of REVs. On the left is an illustration of the REV for an orderly packed bed of spheres. On the right is an illustration of the REV when the porous medium is an orderly consolidated matrix.

same size as one particle cell, that is, one particle and its share of the surrounding free space (see Fig. 1). With this specification, the porous medium characteristics such as the porosity change within one particle cell must be averaged to give a constant. In other words, the cyclic porosity variation within one particle cell should be ignored and an average value should be taken for the whole particle cell region. However, long-range variation of porosity change should be accounted for. Across one particle cell, a monotonic variation may be used to approximate the long-range change.

(b) Product rule:

$$\frac{1}{V}\int_V \phi_1^* \phi_2^* \, dV = \frac{\phi_1\phi_2}{\varepsilon} + \frac{1}{V}\int_V \hat{\phi}_1\hat{\phi}_2 \, dV \qquad (9)$$

where $\hat{\phi} = \phi^* - \phi_\varepsilon$.

(c) Gradient rule:

$$\frac{1}{V}\int_V \nabla\phi^* \, dV = \nabla\phi + \frac{1}{V}\int_{S_i} \mathbf{n}\phi^* \, dS_i \qquad (10)$$

where S_i is the surface area of the solid material in the REV and $\mathbf{n}$ is the out normal of the surface.

(d) Divergence rule:

$$\frac{1}{V}\int_V \nabla\cdot\boldsymbol{\phi}^* dV = \nabla\cdot\boldsymbol{\phi} + \frac{1}{V}\int_{S_i} \mathbf{n}\cdot\boldsymbol{\phi}^* \, dS_i. \qquad (11)$$

For a more complete set of averaging rules, see for example Bachmat and Bear (1986). Following Whitaker (1966), Slattery (1969), Lundgren (1972) and Bachmat and Bear (1986), the volume averaging technique as applied to eq. (7) gives (Du Plessis and Masliyah, 1988, 1991):

the continuity equation:

$$\nabla\cdot\mathbf{v} = 0 \qquad (12)$$

and the momentum equation:

$$Re\,\nabla\cdot(\mathbf{v}\mathbf{v}/\varepsilon) + \varepsilon\nabla p_\varepsilon - \nabla^2\mathbf{v} + F_s\mathbf{v} = 0. \qquad (13)$$

The subscript ε for the pressure is omitted in the literature. F_s is the shear factor or internal flow energy loss coefficient and it contains all the surface and extra volume integrals obtained from the volume averaging procedure. The shear factor is a property of the porous medium and may be determined experimentally or by a theoretical model. Du Plessis and Masliyah (1988, 1991) and Du Plessis (1992) proposed a model in which a representative unit cell of a cubic volume contains one torturous passage having a square cross-section to represent the microstructure of the porous medium and postulated a model for the shear factor. A similar approach was presented earlier by Irmay (1958) to arrive at the macroscopic pressure drop in porous media.

The traditional averaging technique incorrectly imposes that the pressure (Lundgren, 1972) or pressure gradient (Whitaker, 1966; Slattery, 1969; Du Plessis and Masliyah, 1988) inside the solids is zero. Here, one loses the conventional definition of pressure in the porous medium since a fixed value has been arbitrarily assigned to the pressure inside the solid material. Assuming that the solid matrix is incompressible, immobile and not supported by the fluid, the pressure gradient term should be averaged by the following two additional rules:

$$p = \frac{1}{V}\int_V p^* \, dV = \frac{1}{V_0}\int_{V_0} p^* \, dV_0 = p_\varepsilon \qquad (14)$$

and

$$\frac{1}{V}\int_V \nabla p^* \, dV = \nabla p \qquad (15)$$

where V_0 is the volume of the free space in the REV. Equations (14) and (15) indicate that the solid matrix does not share the stress load and forces are only transmitted through the fluid.

By using eqs (14) and (15) for the pressure gradient term, the correct averaged Navier–Stokes equation becomes

$$Re\,\nabla\cdot(\mathbf{v}\mathbf{v}/\varepsilon) + \nabla p - \nabla^2\mathbf{v} + F\mathbf{v} = 0. \qquad (16)$$

In the above equation, the averaged pressure gradient in porous medium is not reduced by the presence of solid materials. When the Reynolds number is zero, eq. (16) can be cast into Brinkman's equation (3). On the other hand, eq. (13) does not reduce to eq. (3) for creeping flows. When the diffusion term is further neglected, both eqs (16) and (13) reduce to the Darcy's law, eq. (1). Hence, the shear factor F of eq. (16) and F_s of eq. (13) can be related under such conditions and are found to differ only in a multiplet of porosity ε. The shear factor based on the Du Plessis–Masliyah model is then given by

$$Fd_{\mathrm{DPM}}^2 = \frac{36(1-\varepsilon)^{4/3}}{\varepsilon[1-(1-\varepsilon)^{1/3}][1-(1-\varepsilon)^{2/3}]} + \frac{\eta^2(1-\varepsilon)}{2\varepsilon[1-(1-\varepsilon)^{2/3}]^2} Re\, d_{\mathrm{DPM}}|\mathbf{v}| \qquad (17)$$

where d_{DPM} is the dimensionless solid material characteristic length of the porous medium. The term η^2 [a value of 2 may be used as per Du Plessis (1992)] is the recirculation factor in the pores or the inertial loss factor in the bends of the model torturous passage. Equation (17) is based on the latest proposal of Du Plessis (1992) which gives a close agreement with the Ergun equation for the pressure drop of flow through a granular bed of porosity $\varepsilon = 0.5$. Above all, eq. (17) establishes a linear dependency of F on the Reynolds number as is observed for flow through porous media.

When the flow is one-dimensional and very weak, i.e. $Re \to 0$, the traditional Darcy's law becomes valid. At this double limit, both Brinkman's equation and the volume averaged Navier–Stokes equation should give the same relationship (Du Plessis and Masliyah, 1988, 1991; Du Plessis, 1992) as that of the Darcy's law. Hence, the porous medium property dependent

d_{DPM} can be related to the permeability k by

$$Fd_{DPM}^2|_{Re=0} = \frac{36(1-\varepsilon)^{4/3}}{\varepsilon[1-(1-\varepsilon)^{1/3}][1-(1-\varepsilon)^{2/3}]} = d_{DPM}^2 \frac{a^2}{k} \quad (18)$$

where the permeability k should be measured without any bounding wall or two-dimensional effects.

Since the volume averaged equation (16) and the original Navier–Stokes equation have the same properties, the numerical treatments should have no differences. However, for high Reynolds number flows, eq. (16) is more stable than the original Navier–Stokes equation.

The governing equations based on eq. (16) for axisymmetrical flows in cylindrical coordinates can be written as

$$\frac{\partial u}{\partial t} + \frac{1}{r}\frac{\partial}{\partial r}\left[r\left(Re\frac{v}{\varepsilon}u - \frac{\partial u}{\partial r}\right)\right] + \frac{\partial}{\partial x}\left(Re\frac{u}{\varepsilon}u - \frac{\partial u}{\partial x}\right) + Fu = -\frac{\partial p}{\partial x} \quad (19)$$

$$\frac{\partial v}{\partial t} + \frac{1}{r}\frac{\partial}{\partial r}\left[r\left(Re\frac{v}{\varepsilon}v - \frac{\partial v}{\partial r}\right)\right] + \frac{\partial}{\partial x}\left(Re\frac{u}{\varepsilon}v - \frac{\partial v}{\partial x}\right) + \left(F + \frac{1}{r^2}\right)v = -\frac{\partial p}{\partial r} \quad (20)$$

$$\frac{1}{r}\frac{\partial (rv)}{\partial r} + \frac{\partial u}{\partial x} = 0. \quad (21)$$

It should be noted that the solution of the velocity field from the volume averaged equations may not be easily compared with experimental data. The flow field represented by the volume averaged equations is in an averaged sense over a representative volume and does not provide information on the local velocity in a pore.

3. A ONE-DIMENSIONAL MODEL FOR PRESSURE DROP IN POROUS MEDIA

The shear factor F needs to be related to the porous medium and fluid properties. Pragmatically, the complexity of the flow rules out any rigorous analytic attempts to resolve the problem. Ideally, one would like to use heuristic arguments to derive an expression for F in terms of universal constants and easily measurable properties of the porous material and the flowing fluid. Such attempts have been made by several researchers in the past. The most successful one is that due to the Kozeny–Carman theory which contains universal constants and easily measurable porous medium properties, d_s' and ε, and fluid properties, ρ and μ. With a properly defined Reynolds number (to account for the inertial effect) and the Forchheimer hypothesis, many correlations have been proposed in the literature. The most notable one is given by Ergun (1952), see eq. (5). However, as MacDonald *et al.* (1979) noted, the relationship provided by the Kozeny–Carman theory does not correlate the experimental data well; hence, it limits the accuracy of the Ergun equation and its derivatives. Another problem associated with the studies in the past is that no relation has been offered for a smooth transition from Darcy's flow (or viscous dominant flow) to Forchheimer flow (or flow with noticeable inertial effect). These two flow regimes have been observed by pressure drop measurements [see, e.g. Fand *et al.* (1988)] and LDV measurements (Dybbs and Edwards, 1984). We shall use heuristic arguments to extend the Kozeny–Carman theory for viscous dominant flows to accomodate for the inertial effect and to relate the Darcy's flow with the Forchheimer flow. In the present section, we shall restrict ourselves to flows with no bounding wall effects.

3.1. *Viscous dominant flow*

Following the Kozeny–Carman theory, we consider a curved flow passage of uniform cross-section and an arbitrary shape to model the pore structure of a porous medium. A sketch of such a flow passage is depicted by Fig. 2.

We assume that the surface (fluid–solid matrix) interactive forces are negligible, that is the traversing fluid consists of a single component or the viscous forces are dominant. The interfacial forces (independent of the flow rate) are only observed under very weak flows. In the limit of creeping flow, Liu and Masliyah (1993) found that the pressure drop in a curved or helical pipe is similar to that in a straight pipe. In analogy to Poiseuille equation, the pressure gradient in a curved flow passage for fully developed flow at zero flow strength can be written as [see also Kozeny (1927) and Carman (1937)]

$$-\frac{\Delta p'}{L} = \frac{16k_1\mu}{d_e^2\tau}u_e \quad (22)$$

where $\Delta p'$ is the pressure drop, L is the apparent length parallel to the main flow, d_e is the equivalent diameter of the passage, u_e is the average (characteristic) velocity in the passage or the characteristic interstitial velocity, τ is the tortuosity of the passage defined as the ratio of the apparent length, as if the passage is straight, to the actual length that the fluid has to travel. The term k_1 is expected to be a universal constant, i.e. not a property of the particular porous medium. For a straight tube (passage), k_1 is a constant that weakly depends on the shape of the passage. For a constant τ and by using the Dupuit's assumption of $u_e = U/\varepsilon$, eq. (22) becomes the Blake–Kozeny equation. Here, U is the superficial velocity. Equation (22) was also given by Carman (1937) as a modified

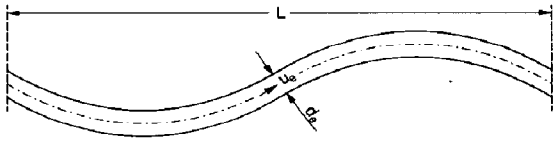

Fig. 2. A sketch of the model curved passage.

Kozeny's equation, however, Carman (1937) and other investigators considered τ to be a universal constant, i.e. independent of the porous structure. For example, Haring and Greenkorn (1970) gave τ^{-1} as 2.25.

Figure 3 shows a representative elementary volume that depicts flow passages in a porous medium. As is shown in Fig. 3, the pores (passages) are interconnected so that fluid mixing among the passages is inevitable and a higher pressure drop than otherwise in a single passage is expected. The curvature and cross-sectional area variation of the passage also result in a higher pressure drop than otherwise for flow through a straight uniform cross-sectional passage. These effects are not all inertial in origin; however, they are more pronounced when the flow rate is increased. If one considers that the passages are parallel and straight, k_1 will have a fixed value. The shape factors for a few types of cross-sectional passages have been given by Carman (1937) and more values can be found in Ward-Smith (1980). The most probable passage cross-section at the pore neck in a packed bed of spheres is shown in Fig. 4. Some relevant values are: $k_1 = 2$ for circular tubes, $k_1 = 1.7784$ for square ducts, $k_1 = 1.6662$ for equilateral triangular ducts and $k_1 = 0.812$ for equilateral concave circular arc quadrilateral ducts [see Fig. 4(b)]. It is clear that the value of k_1 does not change dramatically with the passage shape and the difference in k_1 does not normally exceed 100% for different shapes. In reality, we would expect the value of k_1 to be different from the values given above due to the "imperfections" of the passage.

The characteristic interstitial velocity u_e can be related to the superficial velocity by equating the time required for a fluid element to travel with the superficial velocity U for a fixed apparent length L of porous medium and the time for a fluid element to travel with the characteristic interstitial velocity u_e in the pore for a fixed passage length of L/τ. Hence, we obtain

$$u_e = \frac{A_t}{\tau A_e} U \tag{23}$$

where A_t is the total cross-sectional area normal to the flow and A_e is the free flow cross-sectional area normal to the flow. It should be noted that u_e does not necessarily have to be the average velocity in parallel passages of a uniform cross-section as was considered traditionally.

To obtain the average cross-sectional area ratio, it is reasonable to assume that the porous medium is isotropic. Statistically, the free space for a given direction should be expected to be the same as for the other directions (as one can infer from Fig. 3). Hence, the porosity can be considered as a product of the total three independent directions, i.e.

$$\varepsilon = \frac{A_e}{A_t}\left(\frac{A_e}{A_t}\right)^{1/2} \quad \text{or} \quad \frac{A_e}{A_t} = \varepsilon^{2/3}. \tag{24}$$

The average cross-sectional area ratio as given by eq. (24) is different from that given by Kozeny (1927) and Carman (1937). Their expression for the cross-sectional area ratio is given by

$$\frac{A_e}{A_t} = \varepsilon. \tag{25}$$

Clearly, eq. (25) is valid only when the passages are straight or at least non-intersecting and parallel to the flow. Equation (25) is not valid for an isotropic porous medium.

The equivalent passage diameter d_e is given by

$$d_e = 4\frac{\text{cross-sectional area normal to flow}}{\text{wetted perimeter}} = 4\frac{\text{volume of free space in medium}}{\text{wetted surface area}} = \frac{2\varepsilon d_s'}{3(1-\varepsilon)} \tag{26}$$

where d_s' is the equivalent spherical diameter of the particles or fibres forming the porous structure. It is defined as

$$d_s' = 6\frac{V_P}{S_P} = \Phi_s\left(\frac{6V_P}{\pi}\right)^{1/3}. \tag{27}$$

Here V_P, S_P and Φ_s are the volume, the effective surface area and the sphericity of the particle, respectively.

Difficulty arises as to how to define the tortuosity τ. If the passages are considered uniform in cross-sectional area and/or not interconnected, the definition of τ would have been straightforward. However, the tortuosity is not really a one-dimensional property as two normal directions are used by the traversing fluid when the flow direction at a point is blocked. Since the problem of flow in porous media can be viewed as one-dimensional (or strictly speaking, of two space dimensions but of one flow direction), a two-dimensional model should be adequate in estimating the

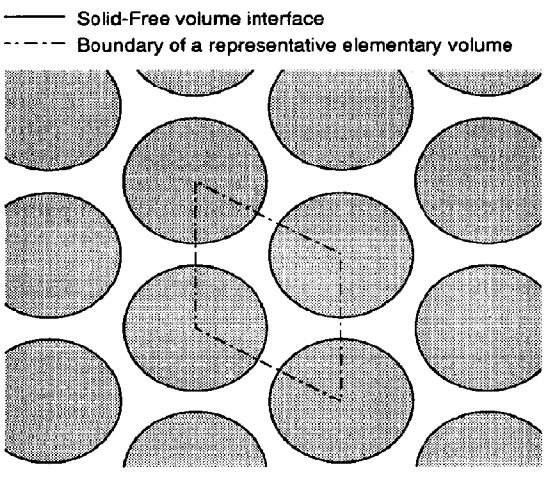

Fig. 3. Flow passages in a representative elementary volume in porous medium.

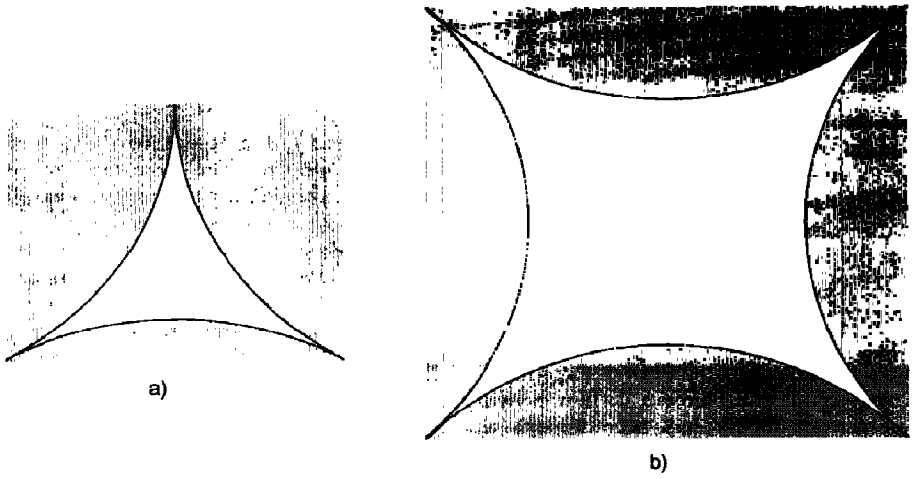

Fig. 4. Equilateral triangle (on the left) and equilateral quadrilateral (on the right) formed by tangent circular arcs.

tortuosity. If the medium is isotropic and two-dimensional, the same arguments can be made in that the porosity is the product of the two equal directions, and we can write

$$\varepsilon = \tau^2 \text{ or } \tau = \varepsilon^{1/2}. \tag{28}$$

Based on their torturous rectangular passage model, Du Plessis and Masliyah (1988, 1991) arrived at two tortuosity equations. They are given as,

for granular beds,

$$\tau_* = \frac{1-(1-\varepsilon)^{2/3}}{\varepsilon} \tag{29}$$

and, for a consolidated medium,

$$\tau_*^3 = \frac{(3\tau_* - 1)^2}{4\varepsilon}. \tag{30}$$

For the purpose of clarity, a subscript * has been added to Du Plessis and Masliyah's models. It can be observed that the tortuosity models given by Du Plessis and Masliyah (1988, 1991) do not yield a zero tortuosity for a completely solid bed. In other words, when $\varepsilon = 0$, $\tau > 0$. However, one would expect τ to be 0 at $\varepsilon = 0$.

The characteristic interstitial velocity can be obtained by substituting eqs (24) and (28) into eq. (23) to yield

$$u_e = U\varepsilon^{-7/6}. \tag{31}$$

Hence, the present model for the characteristic interstitial velocity as given by eq. (31) gives a higher value than the intrinsic phase average interstitial velocity or the interstitial velocity based on the Dupuit's assumption, which is given by

$$u_e = U\varepsilon^{-1}. \tag{32}$$

Owing to the parallel (not interconnected) and uniform cross-sectional area models used by Du Plessis and Masliyah (1988, 1991), their pore velocity is also given by eq. (32).

The final equation for the pressure drop in porous media when the flow is very weak can be obtained by substituting eqs (26), (28) and (31) into eq. (22), leading to

$$-\frac{\Delta p'}{L} = \frac{36k_1(1-\varepsilon)^2\mu}{\varepsilon^{11/3}d_s'^2}U. \tag{33}$$

As a comparison, the equation due to the Kozeny–Carman's theory is given by

$$-\frac{\Delta p'}{L} = \frac{36k_0(1-\varepsilon)^2\mu}{\varepsilon^3 d_s'^2}U$$

where k_0 is the Kozeny–Carman constant (Fand and Thinakaran, 1990). Comparing the above equation with eq. (33), we note that there is a difference in the porosity dependence.

For packed beds, Carman (1937) attempted to determine k_0 with the available experimental data having a narrow range of porosity. From Carman's analysis, we can conclude that with the confining wall effects, $k_0 = k_1/\varepsilon^{2/3} \approx 5.0$ for $\varepsilon \approx 0.39$ and $d_s \approx 0.17$. The exact value of k_1 without any bounding wall effects will be given at a later stage.

It is interesting to note that in Kozeny's and later in Carman's approach, τ was considered as a universal constant and was embedded into the Kozeny–Carman constant. Although it was considered separately by some investigators, the tortuosity was treated as a constant (invariant with porosity). Equation (33) also indicates that the correlations in the literature based on the Kozeny analysis or Blake–Kozeny equation are valid only for a narrow porosity range and cannot be extrapolated to a different range of porosity without loss of accuracy. This behaviour was noted by

MacDonald et al. (1979), who speculated that a better correlation might be obtained by replacing ε^3 in the Ergun equation with $\varepsilon^{3.6}$.

3.2. *Inertial dominated flow*

Up to this point, we have been dealing with creeping flow only. To study the inertial effect on the flow in porous media, we define a pore or particle Reynolds number based on the curved passage model as described in the last section,

$$Re_p = \frac{3d_e\rho u_e}{2\mu} = \frac{d_s'\rho U}{(1-\varepsilon)\varepsilon^{1/6}\mu} \tag{34}$$

where 3/2 is used to make the final form of Re_p simple. When Re_p is very small and below a certain critical value, flow in porous media has been known as Darcy's flow. In the Darcy's flow regime, the pressure drop has nearly a linear dependence on the flow rate and eq. (33) is adequate in estimating the one-dimensional pressure drop in porous media. However, when Re_p is higher than a certain critical value for which Darcy's flow holds, the pressure drop varies significantly with Re_p and shows significant deviation from the linear relation of eq. (33).

Using eq. (33), we can define a modified friction factor

$$f_v = f_m Re_p = -\frac{\Delta p'}{L}\frac{d_s'^2\varepsilon^{11/3}}{\mu U(1-\varepsilon)^2}$$

or

$$f_m = -\frac{\Delta p'}{L}\frac{d_s'\varepsilon^{23/6}}{U^2\rho(1-\varepsilon)} \tag{35}$$

where f_v is the normalized pressure drop factor and f_m is a modified Fanning friction factor. Equation (33) becomes

$$f_v|_{Re_p\to 0} = 36k_1. \tag{36}$$

When Re_p is very large, the pressure drop is dominated by the inertial effect. At this limit, the normalized pressure drop factor may be written as

$$f_{v\infty} = \beta Re_p^n.$$

Here the subscript ∞ denotes large Re_p. For laminar flow in a helical tube, $n = 0.5$. When strong entrance and/or mixing effects are present in a laminar flow, $0.5 \leqslant n \leqslant 1$. Hence it is expected that for flow in porous media, $n \subseteq [0.5, 1]$. It has been shown by many investigators that n is less than unity, especially when the flow rate is very high [$n = 0.9$ by Carman (1937), $n = 0.833$ by Tallmadge (1970), $n = 0.83$ by Jones and Krier (1983) and $n = 0.8$ by Hicks (1970)]. However, it is more customary to assume $n = 1$, which fits experimental data well when Reynolds number is not too high, in other words, the flow is still laminar. When the flow becomes turbulent, the power of n is likely to be less than one.

Another fact presented by the inertial effects is that Re_p alone may not correlate the experimental data well. There are two factors affecting the pressure drop when flow rate is increased. They are: mixing effect and curvature effect. Hence, we can consider that the total inertial term is a summation of the two factors:

$$f_{v\infty} = f_b + f_c \tag{37}$$

where f_b and f_c denote the inertial contributions to f_v from changing passage cross-section area and inter-passage branching (or networking) and from the curvature of the passages, respectively.

If there is only mixing effect (inter-passage connections and variation of passage cross-sectional area), Re_p should be satisfactory in correlating the inertial effects. The excess pressure drop for the mixing effect should be expected to be proportional to Re_p, i.e.

$$f_b = B_b Re_p. \tag{38}$$

For pure curvature effect, the effective Dean number, Dn_e, should be used to correlate the inertial effects instead of Re_p. Here

$$Dn_e = \lambda_m^{1/2} Re_p$$

where λ_m is the characteristic curvature ratio of the passage. To determine the characteristic curvature ratio in a porous medium, the following relationship is sought:

$$\lambda_m = r_0 + r_1\varepsilon^n$$

where r_0, r_1 and n are to be treated as universal constants.

The power n can also be thought of as an index for the multi-dimensionality. Since the flow passages inside the porous media may be regarded as two-dimensional, the value of n should be expected to be 1/2. If porosity was zero, the passages would be extremely curved. That is, $\lambda_m = 1$ for $\varepsilon = 0$, which leads to $r_0 = 1$. When porosity is unity, i.e. free space, the passages become straight. In other words, $\lambda_m = 0$ when $\varepsilon = 1$, which gives $r_1 = -r_0 = -1$. Hence, we obtain

$$\lambda_m = 1 - \varepsilon^{1/2}. \tag{39}$$

Since a fully developed helical flow is not expected to be present in porous media, the pressure drop due to the curvature effect should also be expected to be proportional to the Dean number, i.e.

$$f_c = B_c Dn_e. \tag{40}$$

If we further consider that the curvature and the mixing effects are equally important, i.e. $B = B_c = B_m$, then the total inertial term becomes

$$f_{v\infty} = f_c + f_b = B_c Dn_e + B_b Re_p = B(Re_p + Dn_e). \tag{41}$$

It becomes easier to define a modified Reynolds number, Re_m, based on the above expression that lumps all the inertial effects into one parameter, i.e.

$$Re_m = Re_p + Dn_c = \frac{1 + (1-\varepsilon^{1/2})^{1/2}}{(1-\varepsilon)\varepsilon^{1/6}}\frac{d_s'\rho U}{\mu}. \tag{42}$$

The total inertial term is then simplified to

$$f_{v\infty} = BRe_m. \tag{43}$$

Hence, we have retrieved the relationship for Darcy's flow, eq. (36), and established an appropriate Reynolds number, Re_m, to correlate the inertial effects, eq. (43), for the flow in porous media. In the next subsection, we shall find a correlation capable of predicting the whole range of Re_m for laminar flows.

3.3. *Unified one-dimensional model for viscous and inertial effects*

Similar to the Ergun equation, the normalized pressure drop factor can take the following form:

$$f_v = -\frac{\Delta p'}{L}\frac{d_s'^2\varepsilon^{11/3}}{\mu U(1-\varepsilon)^2} = A + BRe_m. \tag{44}$$

In the limiting cases of small and large Re_m, the corresponding f_v values are given by eqs (36) and (43), respectively. Here, we have

$$B = 0.69. \tag{45}$$

Equation (45) is found satisfactory in representing the experimental data used by Ergun (1952) and MacDonald *et al.* (1979) and it corresponds to $\varepsilon \approx 0.54$ in the Ergun equation (5). Equation (36) gives $A = 36k_1$. The exact value of k_1 shall be defined at a later stage.

For very small Re_m flows, it is evident from experimental data that f_v changes very little with varying Re_m and when Re_m is high, f_v changes linearly with Re_m. This type of a friction loss dependence on the flow rate is due to the influence of the secondary flow in the flow passages and is similar to that presented for flow in helical pipes. The secondary flow in a porous medium can be produced by the mixing action from joining passages and changing passage cross-sectional area and by the curvature of the passage. When the flow in the passage is weak, the secondary flow originated from either mixing or curvature does not give rise to a significantly higher pressure drop than that for a straight uniform cross-sectional passage. Only when the flow is strong can the secondary flow significantly increase the pressure drop in comparison to a straight uniform cross-sectional passage. Liu (1992) and Liu and Masliyah (1993) used the following fRe correlation for flow in a helical pipe:

$$fRe = (fRe)_s + \frac{Dn^{2n}}{C_{Dn}^{2n} + Dn^{2n}} BDn^n$$

where f is the Fanning friction factor, Re is the pipe Reynolds number, $(fRe)_s$ is the value of fRe at $Dn = 0$ or for a straight pipe. C_{Dn} is a constant that signals the importance of the inertial effect and it is proportional to the critical value of Dn for which the inertial effect starts to influence fRe. The term n is the asymptotic order of dependence. It should be noted that fRe is proportional to $Dn^{1/2}$ when Dn is very large, that is, $n = 1/2$. By using the same form of a correlation for porous media and replacing Dn with Re_m, we can obtain the variation of f_v ($= f_m Re_p$) with Re_m. Noting that the asymptotic order of dependence on Re_m is $n = 1$, we obtain

$$f_v = f_m Re_p = -\frac{\Delta p'}{L}\frac{d_s'^2\varepsilon^{11/3}}{\mu U(1-\varepsilon)^2}$$

$$= A + \frac{Re_m^2}{C^2 + Re_m^2} BRe_m \tag{46}$$

where $A = 36k_1$ is the value of f_v at $Re_m = 0$, $B = 0.69$ is the inertial term constant at large Re_m and C can be deduced from experiments. Here C is proportional to the critical Reynolds number that represents the transition from Darcy's region to Forchheimer's region. There is no clear transition between Darcy's flow and Forchheimer's flow. That Darcy's flow is related to Forchheimer's flow in porous media is similar to the Poiseuille flow being related to the centrifugal-force dominated flow in a curved channel.

The parameter C may be estimated as follows. C represents the transition from Darcy's flow to Forchheimer's flow. For a special porous medium built from cylindrical rods, Dybbs and Edwards (1984) observed from their LDV measurements that the secondary flow becomes evident in the pores when the pore Reynolds number, which may be approximated by $2\varepsilon^{7/6}Re_p/3$ in terms of our notations, is about unity. The average porosity reported was around 0.5. Since the onset of strong secondary flow is a signal of a strong inertial effect, we may consider that the critical value for the transition from Darcy's flow to Forchheimer flow is $Re_{pc} \approx 3.4$ (or $Re_{mc} \approx 5.2$) for their particular porous medium. For packed beds, Fand *et al.* (1987) found that the lower bound for Forchheimer's flow to be valid is given by $\varepsilon^{1/6}Re_p = \rho d_s' U/\mu(1-\varepsilon) = 2.3 \sim 5$ for $\varepsilon = 0.35$. Therefore, the critical value for the transition from Darcy's flow to Forchheimer flow to occur is $Re_{mc} = 4.5 \sim 9.8$. Hence, we can note that the transition observed from the pressure drop measurements by Fand *et al.* (1987) agree with the qualitative observation from the LDV measurements by Dybbs and Edwards (1984). By taking a mean value from the experimental results of Fand and Thinakaran (1990), we estimate the critical value for the flow to transit from Darcy's regime to Forchheimer's regime to be $Re_{mc} \approx 7.2$. The proportionality of C with Re_{mc} can be established using the results for flow in helical pipes, where $C_{Dn} = 49$ has been found by Liu (1992) and Liu and Masliyah (1993). The asymptotic correlation for high Dn helical flows given by Hasson (1955) that fits the experimental data best has a lower valid bound of $Dn_c = 21.6$. Hence, we obtain

$$C = \frac{C_{Dn}}{Dn_c} Re_{mc} \approx \frac{49}{21.6} \times 7.2 \approx 16 \tag{47}$$

for the flow in porous media.

4. WALL EFFECT

The presence of a bounding wall containing the porous media presents additional wetted surface area to the fluid flowing within the porous media and affects the properties of the packing (if non-consolidated). More wetted surface area leads to a higher pressure drop and decreases the equivalent diameter of the flow passage. A decrease in the equivalent passage diameter can also be treated as a decrease in the (effective) particle diameter, as depicted by eq. (5). Carman (1937) derived the average porosity variation with spherical particle diameter for maximum dense packings of $d_s \geqslant 2(2-3^{1/2})$ and $d_s = 0.5$. Near the bounding wall in a packed bed, the porosity is likely to be higher. In the radial direction for densely packed beds with an assumed porosity value of unity at the wall, Roblee *et al.* (1958) and Benenati and Brosilow (1962) observed a cyclic variation of porosity with a period close to the particle diameter. However, from the cyclic variation observations one can conclude that the porosity is globally constant when it is averaged within one particle cell. This inferred result confirms the suggestion by Carman (1937) that local porosity variation need not to be taken seriously as long as an average overall porosity is used. It should be noted that channelling (as in fluidized beds) or fingering (as in sedimentation of particles) phenomenon cannot normally occur in a packed bed. When channelling or fingering occurs, it simply means that the porous structure within that region is different and, in particular, the particles have become geometrically ordered in favour of the flow, i.e. no blockage in the flowing direction.

Before we proceed any further, it is necessary to distinguish between a wall effect and the effect of a flow velocity distribution. The wall effect is the effect of the bounding wall surface area on the flow. The geometric confinement posed by the bounding wall is a two-dimensional effect. The two-dimensional effects include global variation of porosity and no-slip velocity condition at the bounding wall. These effects can be treated by the volume averaging technique. The wall effect dealt with in this section does not include the influence on the dynamics of the flow, i.e. the local flow velocity distributions. We deal with the geometrical implication in an overall cross-sectional average sense. For simplicity, the bounding wall shall be considered as a circular tube wall. As an illustration, a diagram of spherical particles randomly packed in a cylindrical tube is shown in Fig. 5.

The first attempt to address the wall effect was made by Carman (1937). He considered that the wall effect on the inertial term is negligible and only the viscous term (Darcy's flow) needs to be corrected. Recent experimental studies showed that Carman's treatment is inadequate, for example, Metha and Hawley (1969) treated the bounding wall surface area exactly the same as the particle surface area. However, no correlation is available that correlates well with experimental data.

4.1. *Wall effect on the viscous term*

Here, we start with the viscous term, i.e. the constant A as affected by the bounding wall. The surface area change may be treated as an effective particle diameter change, i.e.

$$d_p = \frac{d_s'}{C_w} = \frac{Dd_s}{C_w} \tag{48}$$

where d_p is an effective particle diameter used to compute constant A. C_w is the wall correction coefficient and d_s is the dimensionless particle diameter. In previous studies, the bounding wall surface and the particle surface areas were considered to have equal effects on the flow. In this study, we shall treat the bounding wall surface area differently from the par-

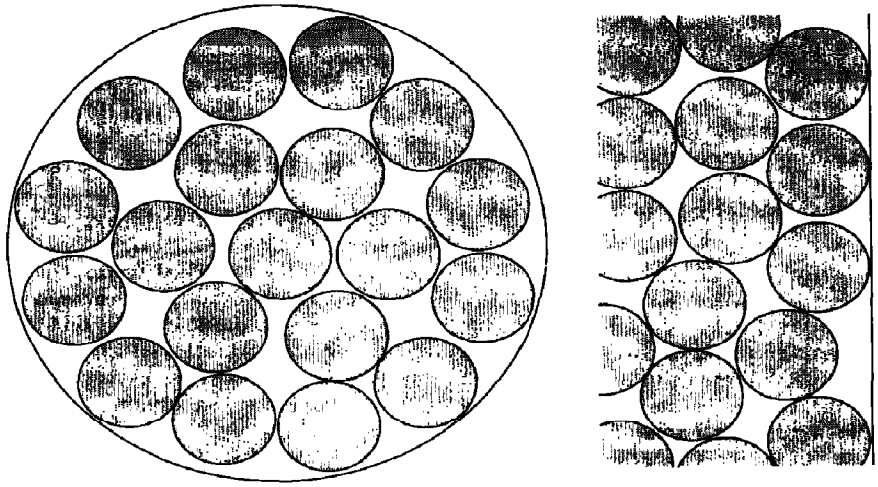

Fig. 5. A sketch of spherical particles contained in a cylindrical tube. On the left is a view of the tube cross-section. On the right is a view along the axial direction.

ticle surface area. The wall surface is relatively flat and the particle surface is convex. The passage would appear more straight near the wall than would be between the particles. Hence, the bounding wall surface area has less influence on the flow than the particle surface area.

Figure 6 depicts the bounding wall together with a spherical particle. The model to be developed is two-dimensional, that is, the bounding wall is a circular tube wall. One unit length (radius of the particle) on the bounding wall surface ($\overline{OW}$) can be projected on the particle surface ($\widehat{OP}$). This projection length of the bounding wall surface will be used to serve as the effective wall surface area. The projection ratio E is given by

$$E = \int_0^1 \sin\alpha \, dy = \int_0^1 (1 - y^2)^{1/2} \, dy = \frac{\pi}{4} \tag{49}$$

where E is the ratio of the projected area on the particle surface to the bounding wall surface area. Hence, we have:

total effective wetted area

$$= \pi DLE + \frac{(1-\varepsilon)LD^2(\pi/4)}{d_s'^3(\pi/6)}\pi d_s'^2$$

$$= \frac{(1-\varepsilon)LD^2(\pi/4)}{d_p^3(\pi/6)}\pi d_p^2 C_w \tag{50}$$

where L is the pipe length and D is the pipe diameter. Equations (48) and (50) lead to

$$C_w = 1 + \frac{\pi d_s}{6(1-\varepsilon)}. \tag{51}$$

The corresponding expressions for C_w are given by Carman (1937):

$$C_{w*} = \left[1 + \frac{2d_s}{3(1-\varepsilon)}\right]^{1/2} \tag{52}$$

and Metha and Hawley (1969) and Reichelt (1972):

$$C_{w*} = 1 + \frac{2d_s}{3(1-\varepsilon)}. \tag{53}$$

In the above two expressions, a subscript * is used to distinguish C_w from our model. Neither of the above two expressions correlate well the available experimental data.

When the wall effect is accounted for, A of eq. (46) becomes

$$A_w = AC_w^2 = A\left[1 + \frac{\pi d_s}{6(1-\varepsilon)}\right]^2 \tag{54}$$

where A_w denotes the constant A as corrected due to the presence of a wall. It should be noted that the mechanism of the wall effect becomes different than that presented above when the particle-to-tube diameter ratio is close to unity. When d_s is very close to 1, the cross-sectional shape of the pores becomes eccentric annulus-like (see Fig. 7) and hence the flow passage shape factor k_1 is increased by over 50% as compared with those for the passages having shapes shown in Fig. 4. When $d_s > 2/3$, the neck to the bulk size ratio of the pores decreases with increasing diameter ratio. Conservatively, eq. (54) can be considered to be valid for $d_s < 0.75$.

4.2. *Wall effect on the inertial term*

The correction on the inertial term due to a bounding wall has been dealt with by Metha and Hawley (1969) and Reichelt (1972). They assumed that the bounding wall and the particle surface areas have the same effect on the inertial term. Their correction factor is given by

$$C_{wi}^* = C_{w*} = 1 + \frac{2d_s}{3(1-\varepsilon)} \tag{55}$$

where C_{wi} is the correction factor for the inertial term. However, Carman (1937) assumed that the wall effect on the inertial term is very small as compared to the viscous term and he neglected the wall effect in the inertial term.

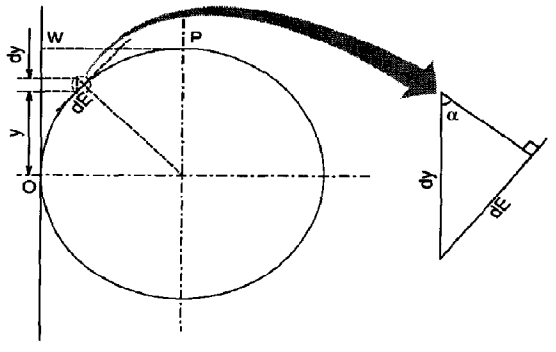

Fig. 6. A two-dimensional projection of the wall-particle diagram.

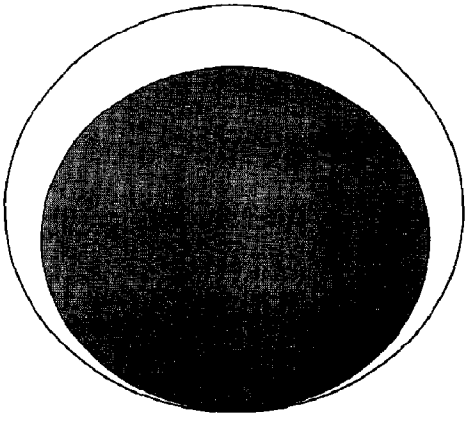

Fig. 7. Cross-sectional view of a packed bed with the diameter ratio greater than 2/3.

Near the bounding wall surface, the fluid has different possibilities for mixing and the flow has less curvature effects. A particle has six faces that can block the flow. Each of the six faces presents a chance for fluid mixing due to the incoming flow towards the face. However, the possibilities of fluid mixing around a particle near the bounding wall are reduced since one of directions has no incoming flow. As the curvature of the flow passage is much reduced near the wall, we may assume that the mixing and the curvature effects are equally affected by the wall. By considering the cross-section of the pipe, we have

$$n_T \propto \frac{\pi}{\pi d_s^2}, \quad n_W \propto \frac{\pi(1 - d_s/2)}{d_s}$$

where n_T is the total number of particles and n_W is the number of particles having one face against the bounding wall. Theoretically, the expression for n_W becomes invalid when $1 < 1.5d_s$. However, the above expressions can be used as an approximation for the entire range of d_s. The wall inertial correction coefficient C_{wi} can be written as

$$C_{wi} = \frac{6n_T - En_W}{6n_T} = 1 - \frac{\pi^2 d_s}{24}\left(1 - \frac{d_s}{2}\right) \quad (56)$$

where E is the effective blocking face area projected by the wall and is given by eq. (49). On the other hand, the presence of the wall leads to a no-slip flow velocity condition. This effect is not to be corrected in this section since it is a multi-dimensional effect and should be taken care of by the volume averaging technique. Hence, the corrected inertial term is given by

$$B_w = BC_{wi} = 0.69\left[1 - \frac{\pi^2 d_s}{24}\left(1 - \frac{d_s}{2}\right)\right] \quad (57)$$

where B_w denotes the constant B as corrected due to the presence of a wall.

5. UNIFIED SHEAR FACTOR AND ONE-DIMENSIONAL PRESSURE DROP EQUATIONS

Based on the proposed model, the final form of the modified friction factor for a one-dimensional flow in porous media with a circular bounding wall can be obtained by replacing A and B in eq. (46) with A_w and B_w, respectively. This leads to

$$f_v = f_m Re_p = A\left[1 + \frac{\pi d_s}{6(1 - \varepsilon)}\right]^2 + 0.69\left[1 - \frac{\pi^2 d_s}{24}(1 - 0.5d_s)\right] Re_m \frac{Re_m^2}{16^2 + Re_m^2} \quad (58)$$

where f_v and f_m are defined by eq. (35), Re_p is defined by eq. (34) and Re_m is given by eq. (36). The above equation is equivalent to Ergun equation while accounting for wall, viscous and inertial effects. Essentially eq. (58) is a one-dimensional pressure drop equation.

The shear factor F in eq. (16) is essentially a local one-dimensional property. At any given point in the porous media, the flow field can be viewed as having one flow direction. The strength of the flow velocity is given by $|\mathbf{v}|$. Hence, eq. (16) can be approximated by

$$-\frac{\Delta p'}{L} = F|\mathbf{v}'|\frac{\mu}{a^2} \quad (59)$$

where $\Delta p'/L$ is the pressure gradient in the flow direction.

Using the definition of f_v, eq. (35), it is possible to relate F in eq. (59) with f_v in which $|\mathbf{v}'|$ is used in place of U. Equations (35) and (59) can be combined to give

$$F = \frac{(1 - \varepsilon)^2}{4d_s^2 \varepsilon^{11/3}} f_v. \quad (60)$$

The modified Reynolds number Re_m should be replaced by a modified local Reynolds number, which is defined by replacing U of eq. (36) with $|\mathbf{v}'|$:

$$Re_v = 2\frac{1 + (1 - \varepsilon^{1/2})^{1/2}}{(1 - \varepsilon)\varepsilon^{1/6}} d_s Re|\mathbf{v}|. \quad (61)$$

Here Re is the pipe Reynolds number.

Hence, the proposed shear factor equation to be used with eq. (16) or eqs (19) and (20) is given by

$$F = \frac{(1 - \varepsilon)^2}{4\varepsilon^{11/3} d_s^2}\left\{A\left[1 + \frac{\pi d_s}{6(1 - \varepsilon)}\right]^2 + 0.69\left[1 - \frac{\pi^2 d_s}{24}(1 - 0.5d_s)\right] Re_v \frac{Re_v^2}{16^2 + Re_v^2}\right\}. \quad (62)$$

Equation (62) together with eqs (19)–(21) can be referred to as a multi-dimensional model for the flow in porous media.

Now, the constant A will be evaluated in this section. A porous medium bed confined in a circular tube is commonly used. Under such conditions, the only averaged velocity component is the axial velocity u. Hence, the volume averaged governing equations may be simplified to one single ordinary differential equation:

$$Fu - \frac{1}{r}\frac{d}{dr}\left(r\frac{du}{dr}\right) = -\frac{dp}{dx} = \frac{(1 - \varepsilon)^2}{8d_s^2 \varepsilon^{11/3}} f_e \quad (63)$$

where f_e is the effective value of f_v or the effective normalized pressure drop factor with multi-dimensional effects.

The boundary and necessary conditions needed for solving the above equation are

$$u = 0 \quad \text{at } r = 1; \quad \frac{du}{dr} = 0 \quad \text{at } r = 0$$

and

$$\int_0^1 ru\,dr = \tfrac{1}{4} \quad \text{(from the non-dimensionalization)}.$$

The local modified Reynolds number can be simplified as

$$Re_v = 2\frac{1 + (1 - \varepsilon^{1/2})^{1/2}}{(1 - \varepsilon)\varepsilon^{1/6}} d_s u Re.$$

It was shown in Section 3.1 that $A = 36k_1 = 36\varepsilon^{2/3}k_0$. The apparent value of k_0 has been given by Carman (1937) for $\varepsilon \approx 0.39$ and $d_s \approx 0.17$ as $k_0 = 5$. Hence, the value given by Carman contains both the wall and the two-dimensional effects. Equation (63) together with eqs (58) and (62) must be used to solve for the viscous term constant, A. In solving eq. (63) together with the boundary and necessary conditions, a central difference method is adequate. A uniform grid of 500 grid points in the radial direction is used. The viscous constant A in eq. (62) is obtained by iteratively solving eq. (63) with the shear factor given by eq. (62). When solving eq. (63), we shall make use of Carman's result. Carman's analysis gave

$$f_v|_{Re=0,\,d_s=0.17,\,\varepsilon=0.39} = 36 \times 5.0\varepsilon^{2/3}\left[1 + \frac{2d_s}{3(1-\varepsilon)}\right] = 114$$

where 5.0 is the value of k_0 and $[1 + 2d_s/3(1 - \varepsilon)]$ is Carman's wall effect correction factor, see eq. (52). The numerical solution gives

$$A = 85.2 \text{ or } k_1 = 2.37. \tag{64}$$

Hence, the final forms of the one-dimensional pressure drop eq. (58) and shear factor eq. (62) contains only the properties of the porous medium and the flowing fluid.

The Ergun equation, when corrected for the wall effects, can be written as

$$f_v = \varepsilon^{2/3}\left\{150\left[1 + \frac{\pi d_s}{6(1-\varepsilon)}\right]^2 + 1.75\left[1 - \frac{\pi^2 d_s}{24}(1 - 0.5d_s)\right]\frac{\varepsilon^{1/6}Re_m}{1 + (1-\varepsilon^{1/2})^{1/2}}\right\}. \tag{65}$$

Correspondingly, the shear factor based on the Ergun equation is

$$F = \frac{(1-\varepsilon)^2}{\varepsilon^3 d_s^2}\left\{37.5\left[1 + \frac{\pi d_s}{6(1-\varepsilon)}\right]^2 + 0.4375\left[1 - \frac{\pi^2 d_s}{24}(1 - 0.5d_s)\right]\frac{\varepsilon^{1/6}Re_v}{1 + (1-\varepsilon^{1/2})^{1/2}}\right\}. \tag{66}$$

Equation (65) is a wall modified one-dimensional Ergun equation and eqs (66) and (19)–(21) can be considered as the wall modified Ergun equation in a multi-dimensional format.

For a special porous medium built from cylindrical rods, Dybbs and Edwards (1984) did not observe any chaotic flow behaviour until their pore Reynolds number reached 300, or in terms of modified Reynolds number, $Re_m \approx 1600$. They estimated the transition to turbulent flow at a pore Reynolds number of 350, which corresponds to $Re_m \approx 1900$. Hence, we may expect eqs (58) and (62) to be valid at least for $Re_m < 1600$.

Figure 8 shows a diagram of the flow regions in a porous medium. The valid region of the model presented in this study is identified as the entire laminar flow regime. In surface interactive force dominant flow regime, the flow has to overcome the interfacial forces independent of flow rate which results in a reverse proportionality between the pressure drop factor and the modified Reynolds number. In the turbulent flow regime, f_v becomes less dependent on Re_m due to the flow becoming partially developed in the pores.

6. TEST OF THE PROPOSED MODEL WITH PACKED BEDS OF MONO-SIZED SPHERICAL PARTICLES

To test the integrity of the model presented in this study, we shall examine a steady incompressible fully

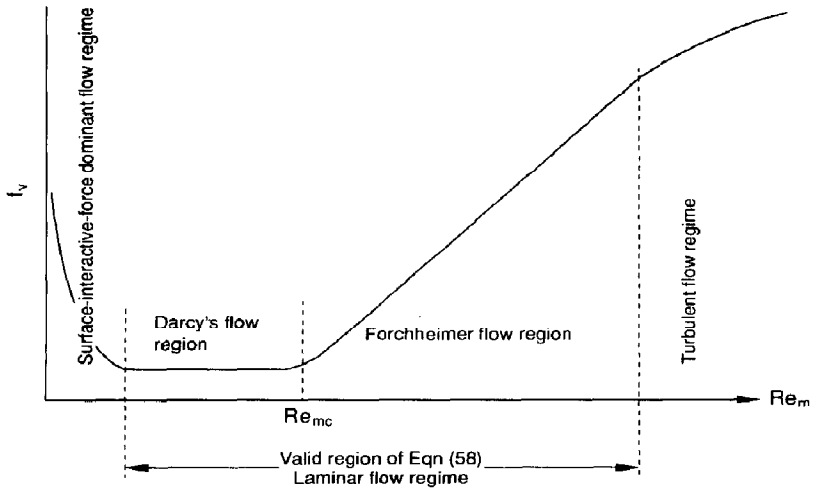

Fig. 8. Flow regions in a porous medium characterized by the modified Reynolds number, Re_m.

developed flow in porous media confined in a circular pipe. There are an abundance of experimental data available in the literature. However, we confine ourselves to the laminar flow regime and insist on mono-sized spherical particles. We shall make use of the latest available data presented by Fand *et al.* (1987) for a packed bed of weak wall effects and Fand and Thinakaran (1990) for a packed bed of strong wall effects. New experimental data are generated in this study to test for the wall effects.

6.1. *Comparison with published experimental data*

Figures 9 and 10 show the normalized pressure drop factor for a densely packed bed of mono-sized spherical particles. The data points are the experimental results taken from Fand *et al.* (1987), where the bed diameter is $D = 86.6$ mm and the particle diameter is $d_s' = 3.072$ mm. One can observe that the current model, referred to as eq. (62), agrees with the published experimental data very well in the whole range of the modified Reynolds number. From Fig. 9, one observes a smooth transition from the Darcy's flow to Forchheimer flow regime. The present one-dimensional model, i.e. eq. (58), showed only slightly smaller f_v value. Hence, the two-dimensional effect for this bed is small. As shown in Figs 9 and 10, the Ergun equation consistently underpredicts the pressure drop. The deviation becomes higher when the flow rate is increased.

Figures 11 and 12 show the normalized pressure drop factor variation with the modified Reynolds number for a packed bed of mono-sized spherical particles having strong wall effects. The experimental data points are taken from the work of Fand and Thinakaran (1990), where the bed diameter is $D = 5.588$ mm and the particle diameter is

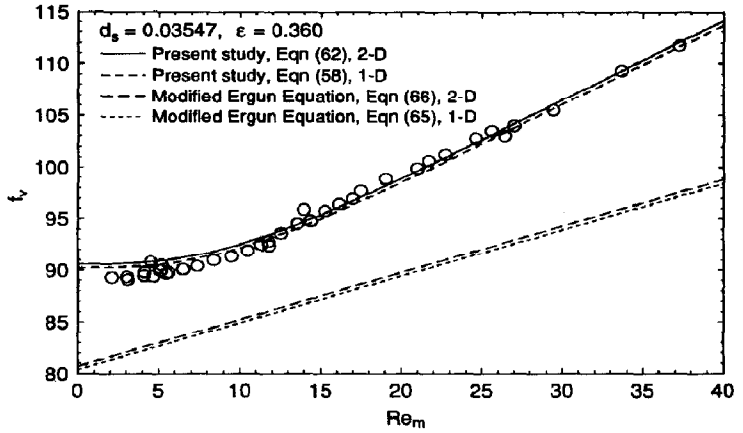

Fig. 9. Variation of pressure drop factor with modified Reynolds number for a densely packed bed of mono-sized spherical particles at low flow rates. The symbols are experimental data taken from Fand *et al.* (1987).

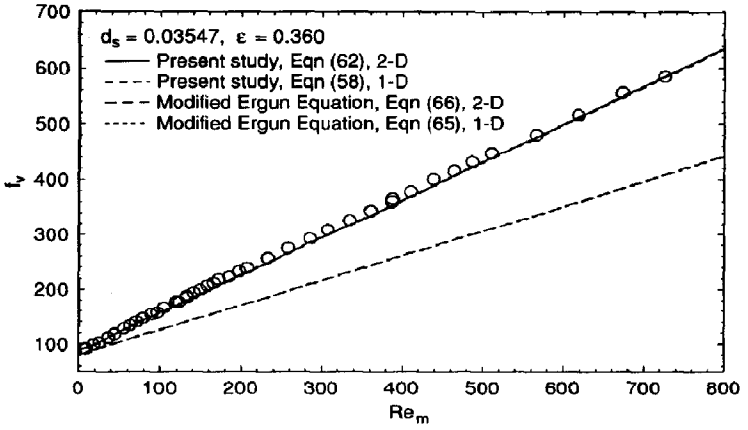

Fig. 10. Variation of pressure drop factor with modified Reynolds number for a densely packed bed of mono-sized spherical particles at high flow rates. The symbols are experimental data taken from Fand *et al.* (1987).

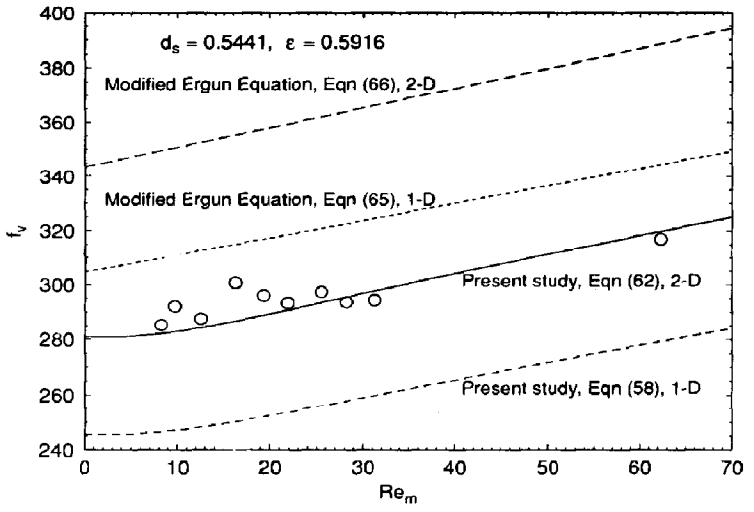

Fig. 11. Variation of normalized pressure drop factor with modified Reynolds number for a packed bed of large spherical particles. The symbols represent experimental data taken from Fand and Thinakaran (1990). Low flow rates.

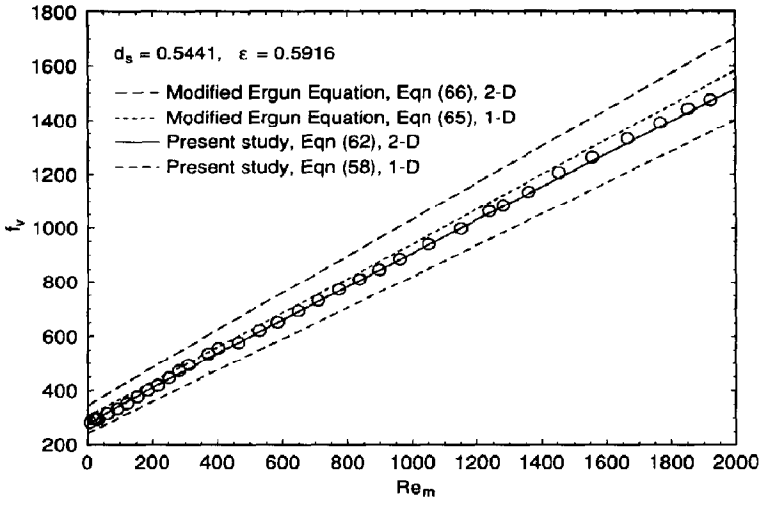

Fig. 12. Variation of pressure drop factor with modified Reynolds number for a packed bed of large mono-sized spherical particles. The symbols represent experimental data taken from Fand and Thinakaran (1990). High flow rates.

$d_s' = 3.040$ mm. Once again, the present two-dimensional model predicts the pressure drop quite well as compared with experimental data of Fand and Thinakaran (1990). For this packed bed, a strong two-dimensional effect is observed. The modified Ergun equation overpredicts the experimental data.

6.2. *Present experimental work*

The experimental apparatus employed in this work consisted of a test section of polyethylene tubing packed with glass beads of narrow size range. The tubing is circular with small elliptical deformation, where the long axis to the short axis ratio is less than 1.05. The particles (glass beads) are nearly spherical, $\Phi_s \approx 1$.

The pipe diameter was indirectly measured by weighing the water inside a known length of the tubing. It was found that the pipe diameter is $D = 4.47$ mm. Two types of particles were used. The particle size and the bed porosity were measured by water displacement test. The procedures are given as follows. First fill half of the test-tube section with

water and then slowly drop a known number of the particles into the tube and gently tap the tube. Measure the increment of the water in terms of the tube length and the bed height. Finally, the porosity and the particle diameter were calculated. In total 150 particles for the small glass beads and 840 particles for the large glass beads were used in the particle size and porosity measurements. The whole procedure has been repeated twice and the results were found to be nearly identical.

Two small pressure taps were drilled into the centre portion of the test section. The test section was 40 cm long. The pressure taps were 10 cm apart for the bed of large glass beads and 3 cm apart for the bed of small glass beads. In the high Re_m range, the working fluid was water. The pressure drop was measured with two U-tube manometers with one filled with a Mariam fluid and the other filled with Mercury. In the low Re_m range, the working fluid was a hydraulic oil (supplied by ESSO) with a density of 860.4 kg/m^3 and a dynamic viscosity of 0.0168 Pa s at 21°C. The pressure drop was then measured by a pre-calibrated differential pressure cell and a U-tube Mercury manometer. In all cases, the flow rate was measured by collecting the effluent liquid from the test section for a given time period.

Figures 13 and 14 show the experimental results as well as the theoretical predictions for the packed bed of large glass beads where $D = 4.47$ mm, $d_s' = 3.184$ mm and $\varepsilon = 0.6007$. One observes that the current two-dimensional model predicts the experimental results fairly well for the entire range studied, $Re_m < 6000$. The deviation between the current two-dimensional model predictions and the experimental data is within 10%. The wall effect modified Ergun equation overpredicts the experimental data in the entire range studied.

Figures 15 and 16 show the experimental data for the packed bed of small glass beads as compared with the theoretical predictions. Here, $D = 4.47$ mm,

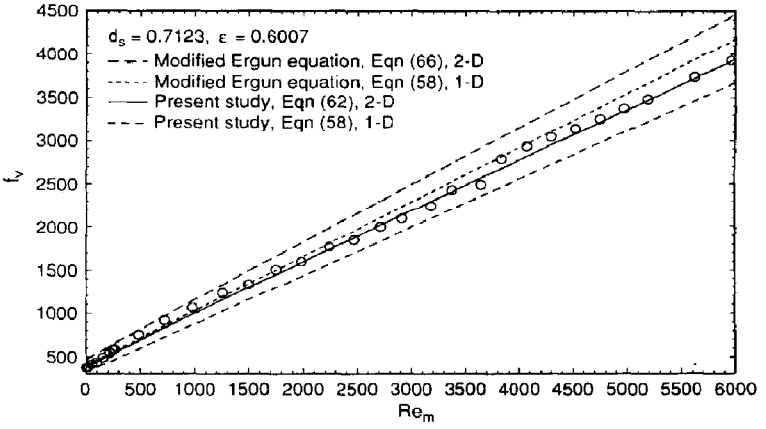

Fig. 13. Pressure drop factor variation with modified Reynolds number for a packed bed having large glass beads in the high Re_m range.

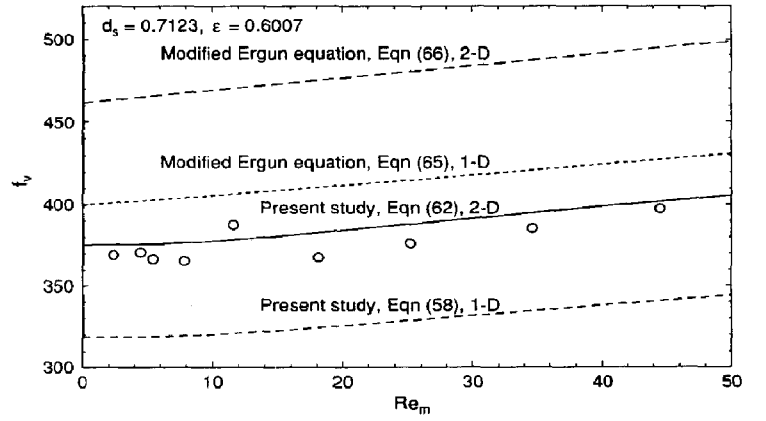

Fig. 14. Pressure drop factor variation with modified Reynolds number for a packed bed having large glass beads in the low Re_m range.

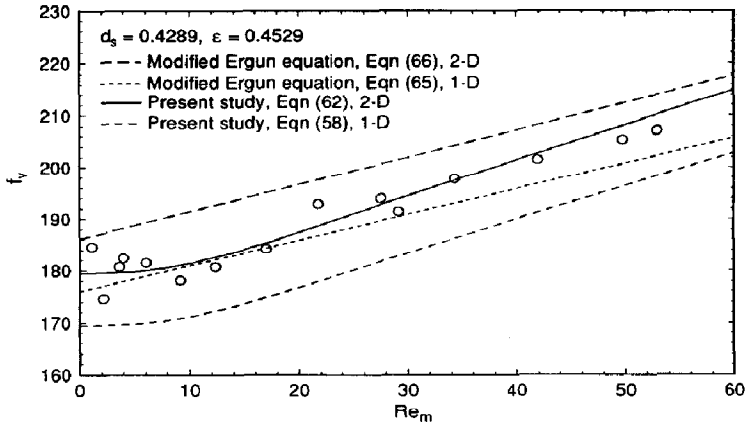

Fig. 15. Pressure drop factor variation with modified Reynolds number for a packed bed of small glass beads in the low Re_m range.

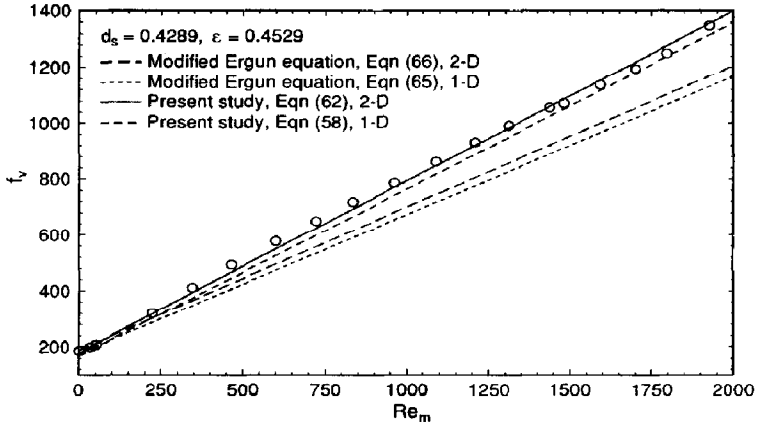

Fig. 16. Pressure drop factor variation with modified Reynolds number for a packed bed of small glass beads in the high Re_m range.

Table 1. Summary of the characteristics of the packed beds used in this study

D (mm)	d_s' (mm)	d_*	ε	Source	C_w^2	C_{wi}	$100\,(f_e - f_v)/f_e$
86.6	3.072	0.03547	0.360	Fand *et al.* (1987)	1.0589	0.9857	0.38
5.588	3.040	0.5441	0.5916	Fand and Thinakaran (1990)	2.8818	0.8371	12.56
4.47	3.184	0.7123	0.6007	Present study	3.7405	0.8114	15.08
4.47	1.917	0.4289	0.4529	Present study	1.9894	0.8614	5.56

$d_s' = 1.917$ mm and $\varepsilon = 0.4529$. We observe that the two-dimensional model of the current study agrees fairly well with the experimental results. The modified Ergun equation predicts the experimental data well in the low Re_m range as is shown in Fig. 15 and underpredicts the experimental data as Re_m is increased (Fig. 16).

Table 1 gives a summary of the packed beds that we made use of in this section. The term $100\,(f_e - f_v)/f_e$ reflects the two-dimensional effects for $Re_m = 0$. A value of zero would indicate no two-dimensional effects. We can observe that the wall effects on the viscous term, C_w^2, range from about 6% for the experimental data of Fand *et al.* (1987) to 274% for the packed bed having $d_* = 0.7123$ as used in the current experimental study. The wall effects on the inertial term, C_{wi}, range from around 1% to 19%. The two-dimensional effects are also significant for the packed beds of large particle to tube diameter ratios. The current model predicts quite well over a wide range of

wall effects. In contrast, the wall modified Ergun equation significantly underpredicts the experimental data at low porosity (Figs 9, 10 and 16) and overpredicts the experimental data at high porosity (Figs 11–14).

7. TEST OF THE MODEL WITH FIXED FIBRE FOAM POROUS MEDIA

To test the proposed model at high porosity, we carried out some experiments with plastic foam porous media. Three types of foams (fine, medium and coarse) were used. The plastic foams were machined into cylinders of 2.55 cm in diameter and 0.305 m in length. The cylindrical foam section was fitted into a plexiglass tube having an inner diameter of 2.55 cm. The working fluid was a hydraulic oil (supplied by ESSO) with a density of 860.4 kg/m^3 and a dynamic viscosity of 0.0168 Pa s at 21°C. Prior to placing the foam into the tube, the foam was soaked in the working fluid for at least one day. The fluid was fed into the tube using a pressurized tank through a rotameter. The pressure drop was measured by a pre-calibrated differential pressure cell. Two small pressure taps, 0.152 m apart, were drilled into the plexiglass and centered in the plastic foam section to allow the reading of the fully developed flow pressure drop within the foam. To guarantee the quality of the experimental results, the flow rate was measured at each data point using the weight of the oil collected at the outlet of the tube and the elapsed collection time. At least two runs were carried out for each foam. The porosity was measured by a Pycnometer after immersing a cubic piece of the foam in the working fluid for one day. The soaked foam cubes were then washed with soap and running water. The foam cube was then used for the porosity measurements. The initial soaking of the foam was performed in order to ensure that if any fibre swelling occurs, the porosity measurements are that of the swollen foam used in the pressure drop measurements.

The fibre diameter was measured by cutting the soaked foam fibre sections and using an image analyser. Since the fibres are very long and "knitted" together in forming the foam, the effective particle diameter is just 1.5 times the fibre diameter according to eq. (27). The measured properties of the plastic foams are tabulated in Table 2. Figure 17 shows

Table 2. The plastic foam properties

Foam	d_s'(mm)	d_s	ε	C_w^2	C_{wi}	$100\,(f_e - f_v)/f_e$
Fine foam	0.167	0.00656	0.9301	1.1007	0.9973	3.37
Medium foam	0.237	0.00928	0.9438	1.1804	0.9962	5.84
Coarse foam	0.348	0.01364	0.9343	1.2292	0.9944	7.04

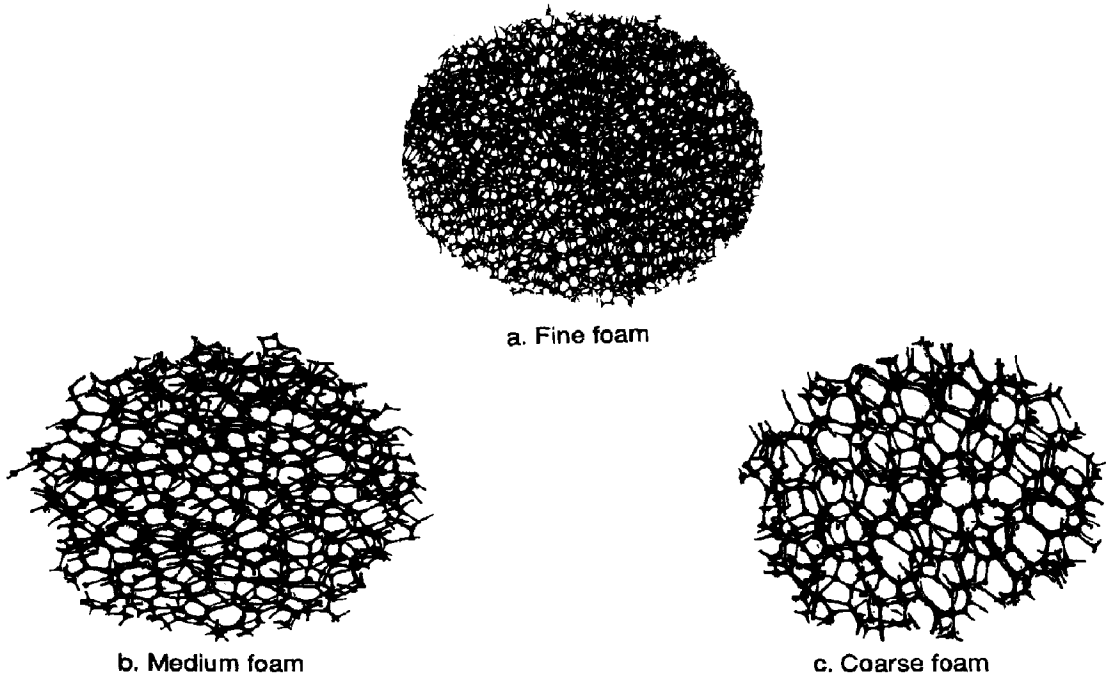

Fig. 17. Cross-sections of plastic foam porous media used in this study.

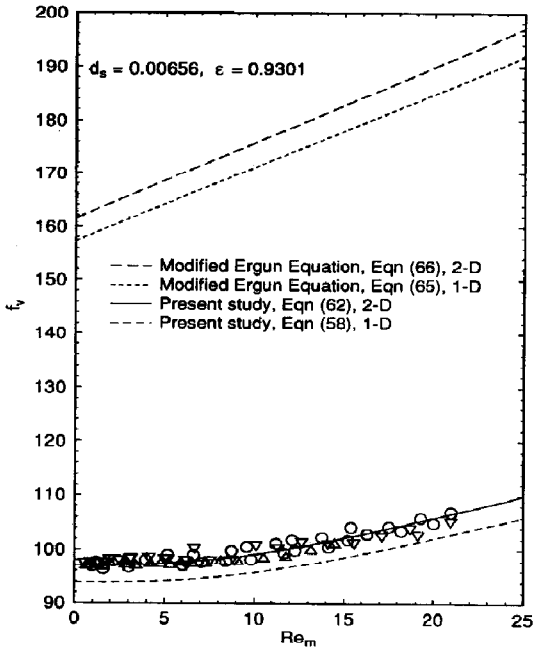

Fig. 18. Normalized pressure drop factor variation with modified Reynolds number for the fine foam.

photographs of the foams used in this experimental study.

Figure 18 shows the calculated pressure drop factor and the experimental values for the fine foam. We observe that the current model predicts the experimental pressure drop both in the Darcy's flow regime, the transition and the Forchheimer regimes. The two-dimensional model gives a much better prediction than that using the one-dimensional model. As is shown in Table 2, the two-dimensional effects for this plastic foam bed are about 3% and the wall effects are about 10% for the various term and 0.3% for the inertial term. This observation may seem rather unexpected as the value of d_s is very small and one would be inclined to suggest that the bounding wall effects are minimal. However, the foam porosity is very high and it leads to higher wall effects. Figures 19 and 20 are for the coarser foams. The discrepancy between the two-dimensional and one-dimensional becomes larger as ε is increased. The wall effects on the viscous term are also higher for the medium and coarse foams as is shown in Table 2. The maximum wall effects are observed for the coarse foam and are 23%. In all the three beds of the plastic foams, the wall effects for the inertial term are negligibly small. Hence, when Re_m is large, the bounding wall effects will become minimal. We should also note that the Ergun equation significantly overpredicts the experimental data.

Figures 19 and 20 show the calculated and experimental results for the medium and the coarse foams. In both cases, the current two-dimensional model predicts the experimental data adequately.

8. CONCLUSIONS AND DISCUSSIONS

Incompressible laminar flow in porous media was studied. The volume averaging technique was revisited and a new averaging approach was presented for the pressure gradient term. The pressure and the pressure gradient term are averaged by assuming that the solid matrix does not share the stress load. Making use of the new averaging method, the volume averaged governing equations reduce to Brinkman's equation when the flow rate is very small.

The Kozeny–Carman theory was reexamined. By linking the one-dimensional flow model with a two-dimensional tortuosity model, pore cross-sectional area change and curvature effects, we arrived at a new semi-empirical equation for the pressure drop in a "one-dimensional" medium. Here, a "one-dimensional medium" implies that the dimension ratio of the porous bed to the grain of the porous medium is very large. The wall effect on the flow in porous media

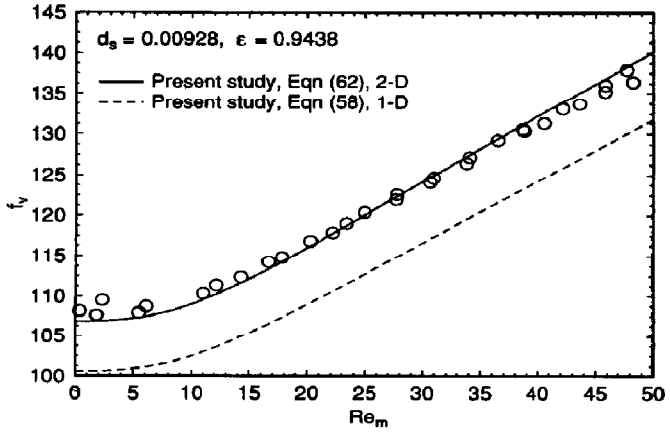

Fig. 19. Normalized pressure drop friction factor variation with flow rate for the medium foam.

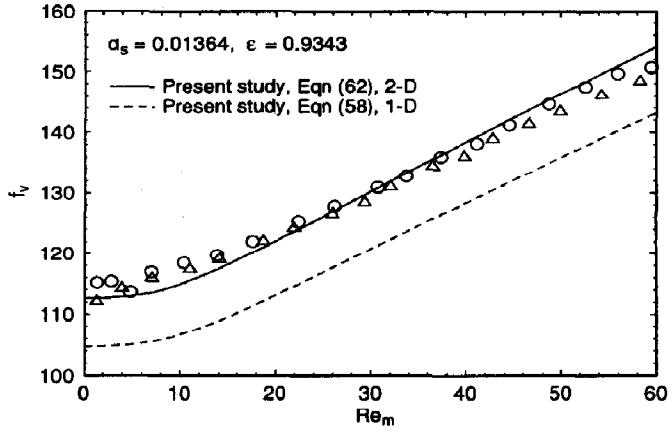

Fig. 20. Normalized pressure drop factor variation with flow rate for the coarse foam.

was incorporated into the friction factor for both Darcy's and Forchheimer's flow regimes. The one-dimensional pressure drop factor is found to be governed by

$$-\frac{\Delta p'}{L}\frac{d_s'^2\varepsilon^{11/3}}{\mu U(1-\varepsilon)^2} = f_v = 85.2\left[1+\frac{\pi d_s}{6(1-\varepsilon)}\right]^2 + 0.69\left[1-\frac{\pi^2 d_s}{24}(1-0.5d_s)\right]Re_m\frac{Re_m^2}{16^2+Re_m^2}$$

and correspondingly, the shear factor for volume averaged Navier–Stokes equation is given by

$$F = \frac{(1-\varepsilon)^2}{4\varepsilon^{11/3}d_s^2}\left\{85.2\left[1+\frac{\pi d_s}{6(1-\varepsilon)}\right]^2 + 0.69\left[1-\frac{\pi^2 d_s}{24}(1-0.5d_s)\right]Re_v\frac{Re_v^2}{16^2+Re_v^2}\right\}$$

where $d_s < 0.75$.

The assumptions made to arrive at the above equations can be summarized as follows: (1) the average free area ratio for a given cross-section of the porous medium is a product of the two out of the three isotropic directions. (2) The tortuosity of the flow passages in the porous medium is an isotropic one-dimensional property out of the flow domain viewed on a plane. (3) The viscous and inertial effects are additive (similar to Forchheimer relation). (4) The inertial effects can be partitioned into two equally important components, namely, mixing and curvature effects. (5) The curvature of the flow passage is a function of the porosity. (6) The mixing and curvature effects are treated in a short developing passage. (7) The wall effect can be incorporated by a change of particle size throughout the bed (Carman, 1937). (8) The mixing and curvature effects are equally affected by the bounding wall.

Comparisons were made with experimental data for both consolidated and unconsolidated porous media of uniform solid size. It is found that the model predicts the experimental data quite well for a wide range of porosity, diameter ratio and Reynolds number.

It should be noted that the volume averaging technique alone is not, strictly speaking, valid for most of the experimental systems studied in this paper. However, we have treated the volume averaged equations as continuous equations and thus applied them to all the systems studied here. The treatment of the bounding wall effects and the uniform porosity approach are able to offset, to a large degree, the errors involved in the application of the volume averaged equations. The mesh size used in solving the equations is not an indicator of the size of the *REV* for the porous medium.

Acknowledgements—Mr Keith Redford assisted in the porosity measurements of the foams and Mr Samir Kayande conducted part of the experiments for the foams. The authors wish to thank Natural Sciences and Engineering Research Council of Canada for financial support.

NOTATION

a	radius of pipe, dimensional
A	viscous term constant
A_e	free cross-sectional area, dimensional
A_t	total cross-sectional area, dimensional
A_w	wall corrected viscous term constant
B	inertial term constant
B_b	mixing effect (inertial) term constant
B_c	curvature effect (inertial) term constant
B_w	wall corrected inertial term constant
C	constant in inertial term signalling the importance of inertial effects
C_w	wall effect factor on viscous term
C_{wi}	wall effect factor on inertial term
d_{DPM}	characteristic porous material length from the Du Plessis–Masliyah model
d_e	equivalent passage diameter, dimensional

d_p equivalent particle diameter with wall effects incorporated, dimensional
d_s equivalent spherical particle diameter, ($= d_s'/D$)
d_s' equivalent spherical particle diameter, dimensional
D pipe diameter, dimensional
Dn Dean number
Dn_e effective Dean number for curvature effect of the flow passage
E effective wall surface area factor
f Fanning friction factor
f_b inertial mixing term, part of f_v
f_c inertial curvature term, part of f_v
f_e apparent f_v, i.e., with multi-dimensional effects
f_m modified friction factor, eq. (35)
f_v normalized pressure drop factor, eq. (35)
F shear factor, dimensionless
F_s shear factor, based on previous studies
k permeability, dimensional
k_0 Kozeny–Carman constant
k_1 flow passage shape factor
L apparent length of porous medium, dimensional
n order of power, constant
$\mathbf{n}$ surface out normal
n_T total number of particles
n_W number of particles near the wall
p' pressure, dimensional
p pressure, dimensionless, eq. (6)
r radial coordinate, dimensionless, eq. (6)
r' radial coordinate, dimensional
r_0, r_1 constants
Re pipe Reynolds number, eq. (6)
Re_m modificd Reynolds number, eq. (42)
Re_p particle Reynolds number, eq. (34)
Re_v local modified Reynolds number, eq. (61)
REV representative elementary volume
S_i solid surface in REV
S_p effective particle surface area, dimensional
u axial velocity, superficial and dimensionless, eq. (6)
u' axial velocity, superficial and dimensional
u_e characteristic interstitial velocity, dimensional, eq. (31)
U superficial cross-sectional average axial velocity, dimensional
v radial velocity, superficial and dimensionless, eq. (6)
v' radial velocity, superficial and dimensional
$\mathbf{v}$ velocity vector, superficial and dimensionless
V volume of REV, dimensional
V_p particle volume, dimensional
V_0 free space volume in REV, dimensional
x, y axial coordinate, along the main flow direction

Greek letters

α constant or angle
β constant
Δ difference
ε porosity
λ_m effective curvature ratio, eq. (39)
μ dynamic viscosity, dimensional
$\check{\mu}$ effective viscosity
ρ fluid density, dimensional
τ tortuosity, or the ratio of the apparent length to the passage average length
ϕ physical variable, dimensionless
$\hat{\phi}$ deviation of the local value from the intrinsic phase average value for ϕ
Φ_s sphericity

Symbol

∇ nabla, gradient operator

Subscripts

b mixing (branch and cross-sectional area change)
c critical value for transition from viscous dominant (creeping) flow to inertial sensitive flow
e effective
i interphase
m modified
p particle
w wall effect
1, 2 index for distinguishing symbol
$*$ distinguishing symbol or based on other models and not in agreement with the current study
ε intrinsic phase average

Superscript

$*$ local value, or distinguishing symbol (based on other models and not in agreement with the current study)
∞ high flow rate

REFERENCES

Bachmat, Y. and Bear, J., 1986, Macroscopic modelling of transport phenomena in porous media. *Transport in Porous Media*, **1**, "1: The continuum approach", 213–240; "2: Applications to mass, momentum and energy transport", 241–269.

Barak, A. Z. and Bear, J., 1981, Flow at high Reynolds number through anisotropic porous media. *Adv. Water Res.* **4**, 54–66.

Bear, J., 1972, *Dynamics of Fluids in Porous Media*. Elsevier, New York.

Benenati, R. F. and Brosilow, C. W., 1962, Void fraction distribution in beds of spheres. *A.I.Ch.E. J.* **8**, 359–361.

Blick, E. F., 1966, Capillary orifice model for high speed flow through porous media. *IEC Process Des. Dev.* (1), 90–94.

Brinkman, H. C., 1949, A calculation of the viscous force exerted by a flowing fluid on a dense swarm of particles. *Appl. Sci. Res.* **A1**, 27–34.

Carman, P. C., 1937, Fluid flow through granular beds. *Trans. Instn chem. Engng* **15**, 150–166.

Coulaud, O., Morel, P. and Caltigirone, J. P., 1988, Modelling of nonlinear effects in laminar flow through a porous medium. *J. Fluid Mech.* **190**, 393–407.

Cvetkovic, V. D., 1986, A continuum approach to high velocity flow in porous media. *Transport Porous Media* **1**, 63–97.

Darcy, H. P. G., 1856, *Les fontaines publique de la ville de Dijon.* Victor Dalmont, Paris. (English translation: Muskat, M.) *Flow of Homogeous Fluids Through Porous Media.* McGraw-Hill, New York, 1937.

Dullien, F. A. L., 1979, *Porous Media, Fluid Transport and Pore Structure.* Academic Press, New York.

Dullien, F. A. L. and Azzam, M. I. S., 1973, Flow rate-pressure gradient measurements in periodically nonuniform capillary tubes. *A.I.Ch.E. J.* **19**, 222–229.

Du Plessis, J. P., 1992, High Reynolds number flow through granular porous media, in *Computational Methods in Water Resources* IX, *Vol.* 2: *Mathematical Modelling in Water Resources* (Edited by T. F. Russel, R. E. Ewing, C. A. Brebbia, W. G. Gray and G. F. Pinder). Computational Mechanics Publications, Boston.

Du Plessis, J. P. and Masliyah, J. H., 1988, Mathematical modelling of flow through consolidated isotropic porous media. *Transport Porous Media* **3**, 145–161.

Du Plessis, J. P. and Masliyah, J. H., 1991, Flow through isotropic granular porous media. *Transport Porous Media* **6**, 207–221.

Dybbs, A. and Edwards, R. V., 1984, A new look at porous media fluid mechanics—Darcy to turbulent in *Fundamentals of Transport Phenomena in Porous Media* (Edited by J. Bear and M. Y. Corapcioglu). Martinus Nijhoff, Dordrecht.

Ergun, S., 1952, Fluid flow through packed columns. *Chem. Engng Prog.* **48**, 89–94.

Fand, R. M., Kim, B. Y. K., Lam, A. C. C. and Phan, R. T., 1987, Resistance to the flow of fluids through simple and complex porous media whose matrices are composed of randomly packed spheres. *Trans. ASME J. Fluids Engng* **109**, 268–274.

Fand, R. M. and Thinakaran, R., 1990, The influence of the wall on flow through pipes packed with spheres. *Trans. ASME J. Fluids Engng* **112**, 84–88.

Forchheimer, P., 1901, Wasserbewegung durch Boden. *Z. Ver. Deutsch Ing.* **45**, 125–127.

Handley, D. and Heggs, P. J., 1968, Momentum and heat transfer mechanisms in regular shaped packings. *Trans. Instn chem. Engng* **46**, T251–T264.

Haring, R. E. and Greenkorn, R. A., 1970, A statistical model of a porous medium with non-uniform pores. *A.I.Ch.E. J.* **16**(3) 477–483.

Hasson, D., 1955, Streamline flow resistance in coils. *Res. Correspondence* **1** s1.

Hicks, R. E., 1970, Pressure drop in packed beds of spheres. *Ind. Engng Chem. Fundam.* **9**, 500–502.

Irmay, S., 1958, On the theoretical derivation of Darcys and Forchheiher formulas, *J. Geophys. Res.* **39**, 702–707.

Jones, D. P. and Krier, H., 1983, Gas flow resistance through packed beds at high Reynolds numbers. *J. Fluid Engng* **105**, 168–172.

Kozeny, J., 1927, Ober Kapillare Leitung das Wassers in Boden. *S. Ber. Wierner Akad. Abt.*, **IIa**, 136–271.

Liu, S., 1992, Laminar flow and heat transfer in helical pipes with finite pitch. Ph.D. dissertation, University of Alberta, Edmonton, Canada.

Liu, S. and Masliyah, J. H., 1993, Axially invariant laminar flow in helical pipes with a finite pitch. *J. Fluid Mech.* **251**, 315–353.

Lundgren, T. S., 1972, Slow flow through stationary random beds and suspensions of spheres. *J. Fluid Mech.* **51**, 273–299.

Ma, H. and Ruth, D. W., 1993, The microscopic analysis of high Forchheimer number flow in porous media. *Transport Porous Media*, **13**, 139–160.

McDonald, I. F., El-Sayed, M. S., Mow, K. and Dullien F. A. L., 1979, Flow through porous media-the Ergun equation revisited. *Ind. Engng Chem. Fundam.* **18**, 199–208.

Metha, D. and Hawley, M. C., 1969, Wall effect in packed columns. *IEC Process Des. Dev.* **8**(2), 280–282.

Nandakumar, K. and Masliyah, J. H., 1982, Laminar flow past a permeable sphere. *Can. J. chem. Engng* **60**, 202–211.

Neale, G., Epstein, N. and Nader, W., 1973, Creeping flow relative to permeable spheres. *Chem. Engng Sci.* **28**, 1865–1874.

Reichelt, W., 1972, Zur Berechnung des Druckverlustes einphasig durchstromter Kugel-ung Zyhlinderschuttungen. *Chemie. Ing. Technol.* **44**(18), 1068–1071.

Roblee, L. H. S., Baird, R. M. and Tierney, J. W., 1958, Radial porosity variations in packed beds. *A.I.Ch.E. J.* **4**, 460–464.

Ruth, D. W. and Ma, H., 1992, On the derivation of the Forchheimer equation by means of the averaging theorem. *Transport Porous Media* **7**, 255–264.

Slattery, J. C., 1969, Single-phase flow through porous media. *A.I.Ch.E. J.* **15**, 866–872.

Tallmadge, J. A., 1970, Packed bed pressure drop—an extension to higher Reynolds numbers. *A.I.Ch.E. J.* **16**, 1092–1093.

Ward-Smith, A. J., 1980, *Internal Fluid Flow: The Fluid Dynamics of Flow in Pipes and Ducts.* Oxford University Press, New York.

Wentz, C. A. and Thodos, G., 1963, Pressure drops in the flow of gases through packed and distended beds of spherical particles. *A.I.Ch.E. J.* **9**, 81–84.

Whitaker, S., 1966, The equations of motion in porous media. *Chem. Engng Sci.* **21**, 291–300.